

Bis-amide and amine bis-amide ligands in M(IV) (M = V, Cr, Mn) based olefin polymerization catalysts: a theoretical study

Timothy K. Firman, Tom Ziegler *

Department of Chemistry, University of Calgary, 2500 University Drive NW, Calgary, AB, Canada T2N 1N4

Received 18 April 2001; accepted 28 July 2001

Abstract

Recent discoveries of active early transition metal olefin polymerization catalysts with positive d-electron counts indicate the potential for a wide variety of new catalysts of this type. To increase our understanding of the influence of d-electrons on these olefin polymerization catalysts, we have used density functional theory methods to model a series of otherwise analogous d^1 V, d^2 Cr, and d^3 Mn systems with an amine and two amide ligands. Second-row analogues are also briefly examined. The preferred geometries of the systems change dramatically in these three different metal systems due to the changes in d orbital occupation. These changing geometric preferences are explained using a valence bond based model of the bonding. The ligands are then linked with ethyl bridges, restricting the possible conformers and changing the catalytic properties dramatically. Both the V and Cr tethered systems are predicted to be good candidates for polymerization catalysts, with the Cr system predicted to be a living polymerization catalyst, with a termination barrier $13.5 \text{ kcal mol}^{-1}$ higher than its insertion barrier. © 2001 Elsevier Science B.V. All rights reserved.

Keywords: Amine; Amide; Vanadium; Chromium; Manganese; Olefin polymerization; DFT; Molecular orbital calculation

1. Introduction

Following the discovery of catalytic olefin polymerization activity of Group IV *ansa*-bridged metallocene systems [1], a great variety of homogeneous transition metal based olefin polymerization catalysts have been discovered. Many d^0 Group III or Group IV metal based systems, with a wide variety of ligands have been found from ‘constrained geometry’ catalysts [2] with a Cp ligand *ansa*-bridged to an amide to the diamide system of McConville and coworkers [3]. A wide variety of these active d^0 polymerization catalysts have been discovered, with a wide variety of metals, from Groups III and IV metals to lanthanides and actinides, with a broad range of ligand systems [4]. Computational modeling of d^0 systems has also progressed rapidly, investigating the reaction mechanisms in detail and exploring varied ligand systems [5]. In a recent series of papers, a unified overview of these d^0 and d^0f^n catalysts based on

density functional theory (DFT) computations was presented [6].

A number of late transition metal ethylene polymerization catalysts have also been developed. Brookhart and coworkers discovered d^8 Ni and Pd olefin oligomerization catalysts which become active polymerization catalysts when modified to include very bulky ligand systems [7]. The steric bulk of these systems inhibits the termination reactions much more strongly than the insertion reactions, as has been demonstrated by theoretical calculations [8]. After a discovery by Bennett, Brookhart et al. and Gibson et al. have developed active catalysts with d^6 Fe and d^7 Co systems [9] which have also been modeled theoretically. A recent review of non-metallocene olefin polymerization catalysis describes the very rapid development of new catalysts based on a wide variety of ligand and metal centers [10].

There are also good catalysts among early transition metals with a few d-electrons. The chromium-based heterogeneous catalysts developed by Union Carbide [11] and Phillips [12] are used to produce a large fraction of the total industrial ethylene production.

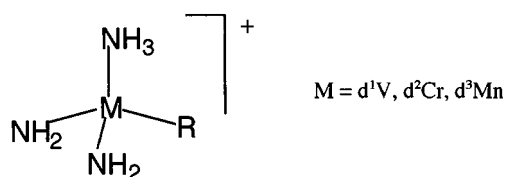
* Corresponding author. Fax: +1-403-289-9488.
E-mail address: ziegler@ucalgary.ca (T. Ziegler).

There has been much recent progress in the development of new homogeneous chromium catalysts, as seen in a recent review by Theopold [13]. Chromium systems with a cyclopentadienyl ligand and either ether [14] or *ansa*-bridged amine [15] ligand(s) have been shown to polymerize ethylene. Ligands forming conjugating six-membered metallocycles, such as ‘nacnac’ (substituted β -diiminate) [16] or salicylaldiminato [17] have been used with chromium and vanadium to form ethylene polymerization catalysts. Very recently, Köhn et al. have found chromium systems with a triazacyclohexane ligand which are trimerization [18] and polymerization [19] catalysts.

With these indications of catalytic potential in compounds with electron counts between zero and eight, we present a computational study of d^1 , d^2 , and d^3 metal systems with nitrogen-based ligands. A previous study [20] of bis-amide systems had found some potential catalysts, which was followed by further exploration with other ligand systems [21]. This study explores systems with two amides and an amine (Scheme 1). The additional ligand changes the catalyst significantly, and the third ligand allows for more options in the restricted ligand conformation by linking the ligands, which we explore with an ethyl-bridged tridentate ligand. We use a valence bond based approach to understand the bonding, an alternative to a model based on molecular orbital theory, as first presented by Dewar 50 years ago [22].

2. Computational details

All calculations were performed with the Amsterdam DFT program package ADF, developed by Baerends et al. [23], using the numerical integration scheme developed by te Velde and Baerends [24]. All atoms were modeled using a frozen core approximation. V, Cr, and Mn were modeled with a triple- ζ basis of Slater type orbitals (STO) representing the 3s, 3p, 3d, and 4s orbitals with a single 4p polarization function added. Mo, Ru, and Pd were similarly modeled with a triple- ζ STO representation of the 4s, 4p, 4d, 5s, and a single 5p polarization functions. Main group elements were described by a double- ζ set of STO orbitals with one polarization function (3d for C, N and 2p for H) [25]. A set of auxiliary s, p, d, f, and g STO functions, centered on all nuclei, was used in order to fit the



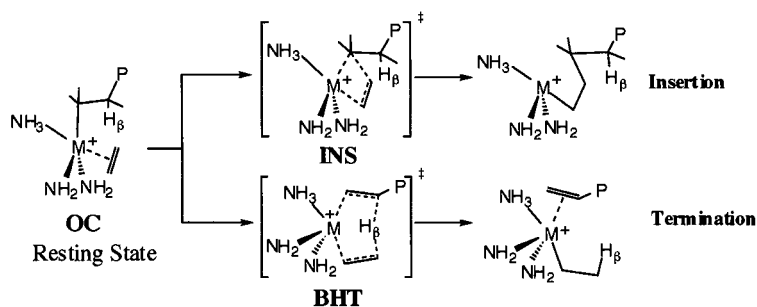
Scheme 1. Initial model systems.

molecular density and present Coulomb and exchange potentials accurately in each SCF cycle [26]. In each case, the VWN local exchange-correlation potential [27] was used, augmented with electron exchange functionals according to Becke [28] and correlation corrections according to Perdew [29] in a self-consistent fashion. This method, commonly referred to as BP86 in the literature, has proven to be reliable for both geometries and energetics of transition metal systems similar to those used here [30]. Jensen and Bøvre have shown that the BP86 functional gives results in excellent agreement with the best wave function based methods available today for olefin insertion in titanium systems, similar to the complexes discussed here [31]. All computations were performed in a spin-unrestricted fashion except for the singlet Mo, Ru, and Pd systems, for which spin-restricted calculations were done. None of the calculations used symmetry. First-order scalar relativistic corrections [32] were added to the total energy of all systems. A perturbative relativistic approach has been shown to be sufficient for first row systems by Deng et al. [33]. All geometries were converged to a maximum force of $0.001 \text{ hartree } \text{\AA}^{-1}$ or hartree radian $^{-1}$. For insertion, transition states were located by optimizing all degrees of freedom except for a chosen reaction coordinate (the forming carbon–carbon bond), iterating until the local maximum along that coordinate was found. For β -hydride transfer, transition states were found using a standard stationary point search to a Hessian with a single negative eigenvalue. Orbital plots were all made with the ADFPLT 1.1 program [34] and all depict at the 0.05 a.u. isosurface.

3. Results and discussion

3.1. Elementary reaction steps and terminology

We depict in Scheme 2 the elementary steps in olefin polymerization. In the first step toward chain propagation, an ethylene binds to the precursor to form an olefin-bound, π complex (OC). The energy difference between the precursor and the olefin complex OC is labeled E_{OC} . The next step in the propagation path is the insertion of the olefin into the metal–alkyl bond via the insertion transition state, which we label INS. The energy difference between the OC and INS structures is the insertion barrier, or ΔE_{INS} . A substantial olefin binding enthalpy, or uptake energy, is needed to overcome the intrinsic entropic penalty of a bimolecular reaction, and a low insertion barrier is required for reasonable catalytic activity. Reactions that terminate the growing polymer chain must also be considered, so we consider β -hydride elimination (BHE) and β -hydrogen transfer (BHT) to the monomer. As in a previous study of compounds using these metals and spin states



Scheme 2. Elementary steps in olefin polymerization.

[20], we found that BHE was substantially energetically unfavorable, either with a thermodynamic barrier higher in energy than the BHT mechanism, or in several cases no minimum was found for the presumed hydride product. The primary termination mechanism is therefore via a BHT path, with a barrier equal to the energy difference between the OC minimum and the BHT transition state, or ΔE_{BHT} . In order to achieve high molecular weight polymers, the insertion barrier must be well below all possible termination barriers.

3.2. $(\text{NH}_3)(\text{NH}_2)_2\text{MR}^+$ systems

We begin our study by modeling with a simple system composed of two amides and an amine. This small system has the obvious advantage of speed of computation, and its relative lack of steric interactions and its conformational flexibility make it ideal for the study of electronic effects. As we go from the d^1 V, to the d^2 Cr, and to a d^3 Mn system, the electronegativity of the metal changes only by a small amount; the largest change to the system results from the number of unpaired electrons. In molecular orbital terms molecular geometry will distort to lower the energy of each of the singly occupied molecular orbitals (SOMOs), as has previously been discussed in detail for the similar $\text{M}(\text{NH}_2)_2(\text{C}_2\text{H}_5)^+$ series. [20] Another way to consider these systems is using a valence bond approach [35] in which the metal forms polarized covalent bonds with the ligands. The covalent bonding orbitals must be mutually orthogonal, which implies that two covalent bonds will avoid pairwise overlap or pay an energetic penalty due to the loss of bonding. In cases where there are insufficient metal bonding orbitals available for all the ligands to bind to the fullest extent, the weaker interactions (in this case, the metal–amide π bonds and the metal–amine bond) will share the metal bonding orbitals or may not be bound at all. The number of SOMOs in the system influences the geometric shape and energetics of these systems by reducing the number of bonding interactions the transition metal can form with the ligands. Six valence (3d and 4s) orbitals are usable [35] by these metals for covalent bonding, so the

d^1 vanadium complex thus can have five bonding interactions (six minus the partially occupied SOMO), the chromium four and the manganese only three.

The shapes of the precursor catalysts are shown in Fig. 1. The vanadium structure has planar NH_2 groups with strong π bonding while the Mn has pyramidal

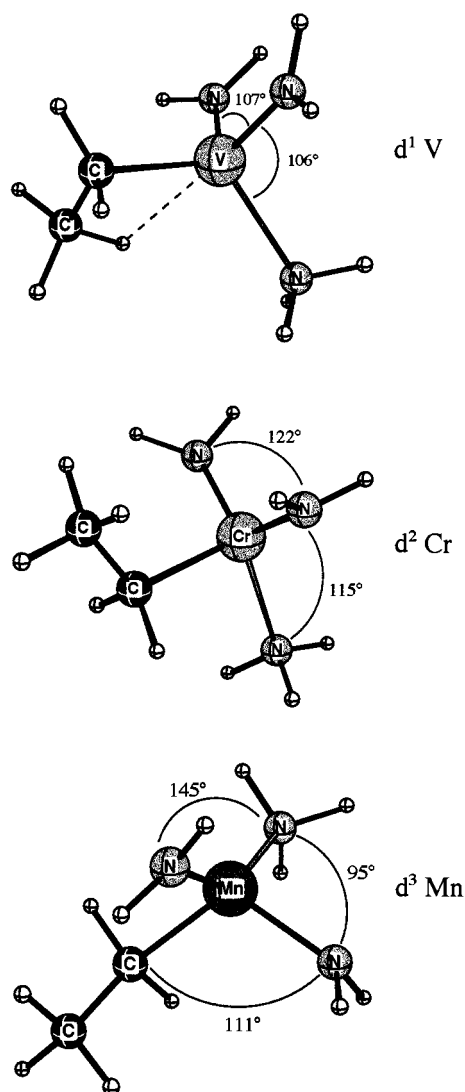


Fig. 1. Calculated shapes of model precursor catalyst systems.

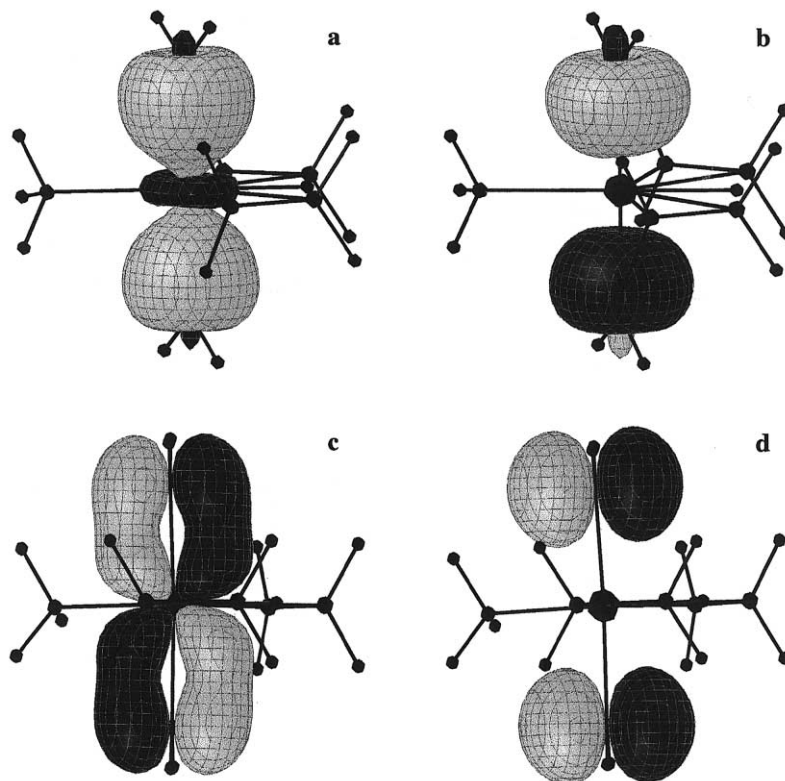


Fig. 2. Linear combinations of Boys-localized orbitals, forming *trans*-amide bonds (a and c) to chromium and electron pairs localized on the ligands (b and d).

NH₂ groups with greatly reduced π bonding. Chromium also has planar NH₂ groups π bonded to chromium, but the two π interactions are in the same plane; because they are coplanar, the two π interactions can share a single metal bonding orbital.

An example of this sharing of metal orbitals is shown in Fig. 2. These are orbitals from the β -hydride transfer transition state of chromium, chosen because a system with a *trans*-orientation of the amide ligands is graphically clearer. The four orbitals depicted are linear combinations of Boys-localized orbitals [36] of *trans*-NH₂ groups. Boys localization results in four banana-shaped bonds, two to each ligand; a 2×2 unitary transformation of pairs of these orbitals gives the familiar σ - and a π -bond to each of the ligands. Taking this a step further, an additional 2×2 unitary transformation to combine the two *trans*- σ bonds reveals a single orbital binding the metal to both ligands and an orbital of a ligand-localized lone pair distributed on both of the amides, as depicted in Fig. 2. An additional transformation to combine the two π orbitals shows an analogous result: an orbital with a strong π bond to the metal and an orbital of a lone pair split between the two *trans*-ligands. This bonding, particularly in the case of *trans*- σ -type orbitals, is somewhat analogous to main group three-center four-electron hypervalent interactions [35]. The chromium only uses two orbitals to

form all the bonds with these two ligands, as there is but a single σ bonding d_{z^2} orbital binding both amides and a single π bonding d_{xz} orbital also binding to both amides. In general, a transition metal will use a single σ orbital to bind both of a pair of ligands *trans* to one another, and a single π orbital to bind two coplanar π bound ligands. Such interactions are much more common in transition metal compounds than in main group analogues, partly because both d and s orbitals are symmetric with respect to inversion, so any bond formed from them must extend equally in both directions along a given axis, unlike the more unidirectional sp hybrids.

The differing shapes shown in Fig. 1 result from the restriction in the number of orbitals. The vanadium structure has double bonds to both amides, and also a β -agostic hydride interaction. Chromium, with one fewer open binding orbital available, lacks a β -agostic interaction and its two amide π interactions are coplanar, sharing an orbital. The manganese structure has again one fewer interaction, causing the loss of the last amide π interaction, as seen by the pyramidalization of the amides.

3.2.1. Ethylene binding

The first step toward polymer growth is the binding of an ethylene monomer to the transition metal. The

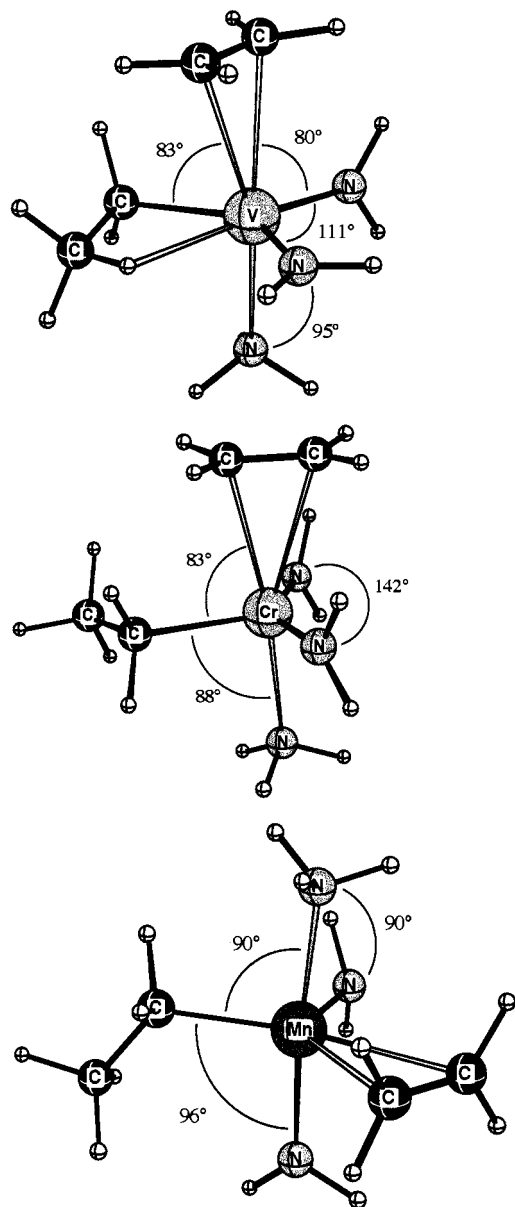


Fig. 3. Shapes of ethylene adduct systems, OC.

Table 1
Calculated reaction enthalpies for generic model systems (in kcal mol⁻¹)

Model catalyst	Energy with respect to reactants			Barrier heights	
	E_{OC}^a	E_{INS}^\ddagger ^b	E_{BHT}^\ddagger ^c	ΔE_{INS}^\ddagger ^d	ΔE_{BHT}^\ddagger ^e
V(NH ₂) ₂ (NH ₃)C ₂ H ₅ ⁺	-3.0	+13.3	+13.4	+16.3	+16.4
Cr(NH ₂) ₂ (NH ₃)C ₂ H ₅ ⁺	-5.2	+7.3	+14.4	+12.5	+19.6
Mn(NH ₂) ₂ (NH ₃)C ₂ H ₅ ⁺	-5.4	+8.2	+14.6	+13.6	+20.0

^a Energy of olefin coordinated compound with respect to ethylene and precursor.^b Energy of ethylene insertion TS with respect to ethylene and precursor.^c Energy of β -hydride transfer TS with respect to ethylene and precursor.^d Barrier height — energy of ethylene insertion TS with respect to OC.^e Barrier height — energy of β -hydride transfer TS with respect to OC.Table 2
Energy penalty of rotation of the planer amide groups in OC

H-N-V-N	Out of plane ^a	In Plane ^b	0° torsion	90° torsion	180° torsion
Out of plane ^a	+1.3	+0.04			
In plane ^a	-	+10.1			
H-N-Cr-N					
Out of plane ^a	+5.6	+8.4	Out of Plane	In Plane	
In plane ^b	-	+0.9			

Energies in kcal mol⁻¹ with respect to unconstrained minimum for each metal. 'In Plane' and 'Out of Plane' refer to the metal–nitrogen π bond and the N–V–N plane.

^a H–N–M–N torsions are constrained to 0° and 180° to constrain the π bond of that amide to be perpendicular to the N–M–N plane.

^b H–N–M–N torsions constrained to 90° and -90° constrain the π bond of that amide to be in the N–M–N plane. If both amides are In Plane the two π bonds are coplanar.

addition of an ethylene to these systems results in a five-coordinate compound with an approximate trigonal bipyramidal shape. The structures are shown in Fig. 3.

The E_{OC} column of Table 1 shows the energy difference between the precursor and the olefin adduct for the systems studied. All three of these initially studied systems have small uptake (E_{OC}) energies, smaller than the enthalpy penalty expected for this bimolecular reaction. The entropic penalty of this addition was calculated to be 13.7 kcal mol⁻¹ for the d¹ V system at 300 K using vibrational data and an harmonic oscillator, rigid-rotor, ideal gas approximation; the penalties for other systems are expected to be similar. As in the four-coordinate precursor systems, the d¹ V system has two independent π bonds, the Cr two overlapping ones, and the Mn has pyramidal amides due to lack of π bonding. To further illustrate the importance of the relative alignment of the amide π bonds, we examine

the consequences of constraining the rotation of the amide groups with respect to the other amide, with the results displayed in Table 2.

(The manganese system is not listed, as the amides are far from planar and these constraints enforce planarity.) If all the H–N–M–N torsions are constrained to $\pm 90^\circ$, the two amide π orbitals are in plane and overlap, which requires a 10 kcal mol⁻¹ penalty in the V case but is near the minimum in the Cr case. If one or both of the amide π bonds leave the N–M–N plane, as in cases with torsions of 0 and 180°, the V system is very near its minimum energy, while in the Cr case there is a significant penalty for forcing the π orbitals out of alignment. The σ orbitals also play a role: the more covalent bonds, particularly the metal–ethyl bond, will avoid overlap with the other metal orbitals, while the weak σ interactions such as the bond to the amine tend to share metal orbitals, as the σ orbitals in Fig. 2 above.

During the transition states the metal environment changes significantly, thus altering the preferred orientation of the ligands. This change in preferred orientation can be used to help in the rational design of

catalysts, for example, by choosing ligands which are particularly stable in the insertion transition state while destabilized in the termination transition state (BHT, for these systems.) In Section 3.4 we will examine the changes caused by using a chelating ligand, limiting the rotation and orientation of the individual nitrogen groups.

3.2.2. Insertion transition state (chain propagation)

The next step toward polymer growth is the formation of a new carbon–carbon bond. Fig. 4 shows the localized orbitals [36] directly involved in this process for the Cr case.

The orbitals in the ground state ethylene adduct system depicted on the left show a strong metal–ethyl bond and a weaker metal–ethylene π bond. The amide group is oriented along the axis of the metal–ethylene bond, so that the two weak σ orbitals share an orbital. On the right are the two analogous orbitals during the insertion transition state. The metal–alkyl σ bond breaks as the new C–C bond is forming. As this bond forms, the lower right orbital depicts the olefin shift from an η^2 - to an η^1 -binding mode to the metal. In this

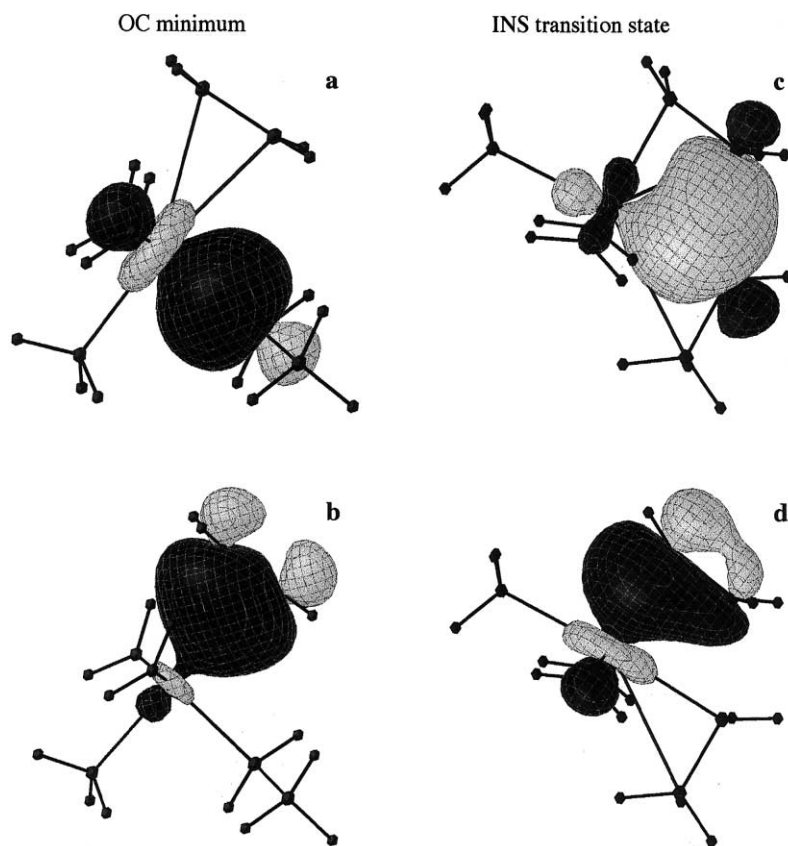


Fig. 4. Localized orbitals in the insertion TS (chromium pictured).

a In the OC minimum: the localized Cr-alkyl orbital

b In the OC minimum: the localized Cr-ethylene orbital

c In the INS transition state: the Cr-alkyl bond is shifting to form a C–C bond

d In the INS transition state: the Cr-ethylene bond is becoming a Cr-alkyl bond

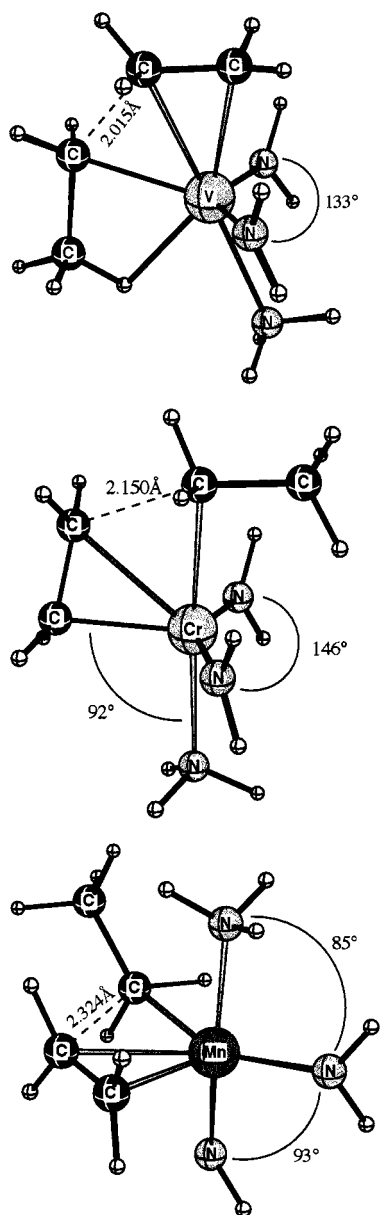


Fig. 5. Shapes of INS, the insertion transition state.

case the other three ligands rearrange prior to the insertion to place the amide *trans* to the breaking Cr–C; this is consistent with its preference for orienting opposite weak bonds. The insertion process may also require a rotation of the alkyl and the ethylene before insertion can occur.

During the insertion transition state, the transition metal must form an additional strong covalent bond to the ethylene. This additional bond changes the preferred orientation of the amide ligands as shown in Fig. 5.

The amides in the d^1 vanadium system have rotated to align their π bonds, a rotation that required $10.1 \text{ kcal mol}^{-1}$ in the ground state but is minimal here. The extra V–C bond forming in this transition state makes

the sharing of these orbitals necessary. The Cr and Mn compounds both pseudo-rotate to change so that the ligands are axial in their trigonal bipyramidal shapes. The significance of these changes in preferred shape between the minimum and the transition state becomes apparent when considering chelating ligands which prevent free rearrangement between these shapes. The barrier heights of the insertion process (ΔE_{INS} values in Table 1) for these three initial complexes are each too high for rapid insertion to occur. Changing to a chelating ligand will effect the energies of the OC systems differently than it will the INS resulting in different barrier heights, as will be seen in Section 3.4.

3.2.3. β -Hydride transfer transition state (chain termination)

Finally, the polymer chain stops growing as a result of a termination step, in this case via a β -hydride transfer transition state. A hydrogen atom on the β carbon of the growing polymer chain migrates to the monomer, which can be followed by the elimination of the old polymer chain as an alkene. The energy penalty of this process comes primarily from the breaking of the strong C–H bond, thus in the transition state structures the transferring hydrogen is located midway between the two carbon atoms. In each of these systems, the transition metal is closely involved, stabilizing the transferring hydride with a strong σ -bonding interaction. This four-center interaction, consisting of a hydride interacting with two carbons and with the transition metal, is shown in localized orbital form for the Cr case in Fig. 6.

In this pseudo-octahedral transition state, the two alkene-like ligands and the transferring hydrogen must be along a meridian, which is facilitated by the other three ligands conforming to fill the other median of the pseudo-octahedron. The shapes formed by the three metals studied are found in Fig. 7.

Both the Cr and Mn have a pseudo-octahedral shape, the principle difference between the two being the expected lack of a π interaction in the Mn case. In these two cases, both amides share a single σ metal orbital, as depicted for the Cr example in Fig. 2. This becomes favorable both because of the preferred pseudo-octahedral shape and the extra metal–hydrogen interaction reducing the number of other metal bonding orbitals by one. The vanadium transition state avoids the shared σ orbital by keeping the three nitrogen-based ligands in a pseudo-facial arrangement, but does align the amides to share that orbital. While this non-octahedral shape may be mildly sterically disfavored, the vanadium system had a β -hydride agostic interaction in its the global minimum structure, facilitating the formation of this transition state with respect to the other two metals. The energies required for this termination transition state are listed in Table 1. All three metals have similar termination barriers. The termination barriers for Cr

and Mn are considerably higher (by 6–7 kcal mol⁻¹) than the insertion barriers, which is particularly notable considering the lack of steric bulk in these systems, as sterically unhindered model systems often have low termination barriers, often lower than the insertion barriers [6]. Steric bulk in ligands is usually necessary to raise the termination barrier while having less of an effect on, or sometimes even reducing, the insertion barrier [9]. These high termination barriers will become much more important after modifications are made to decrease the insertion barrier and increase the binding energy of the ethylene.

3.3. Mo (*d*²) Ru (*d*⁴) and Pd (*d*⁶) analogue systems

A series of calculations was carried out on some second-row systems. All were found to be low spin, with one, two, and three metal orbitals doubly occupied

rather than singly occupied, analogous to the V, Cr, and Mn systems, respectively. It was hoped that the second row would have larger uptake energies due to stronger metal–ligand bonding. The results are presented in Table 3.

Unfortunately, the results were not encouraging. In every case, the insertion barrier was high, and termination barriers were generally only slightly higher, or in one case lower, than the corresponding insertion barriers. The uptake energies did improve, but the high insertion barriers indicate that these combinations of ligands and metals are not a promising area to seek new catalysts.

3.4. Chelating ligand systems

The first-row transition metal systems we studied initially were modified by the addition of ethyl bridges

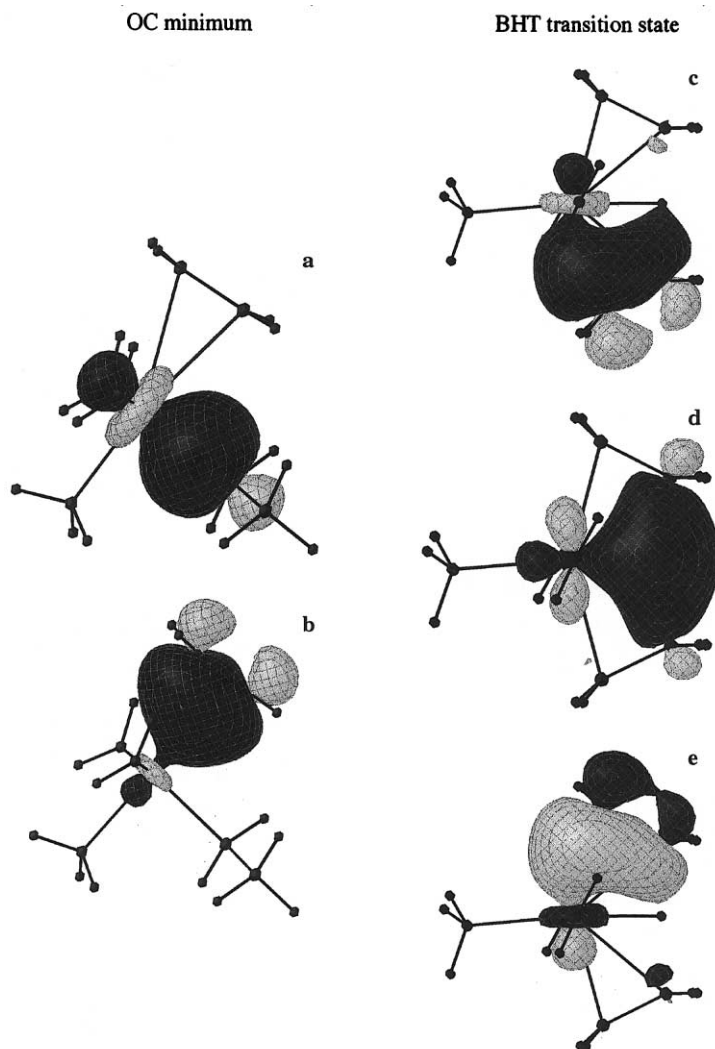


Fig. 6. Localized orbitals in the β -hydride transfer TS (chromium pictured). **a.** σ bonding orbital to alkyl in OC. **b.** Cr-ethylene orbital in OC. **c.** η^1 σ bond **a** is becoming an η^2 π bond. **d.** A β -hydride orbital intermediate between two C, with a new and significant interaction with the metal. **e.** η^2 π bond **b** is becoming an η^1 σ bond.

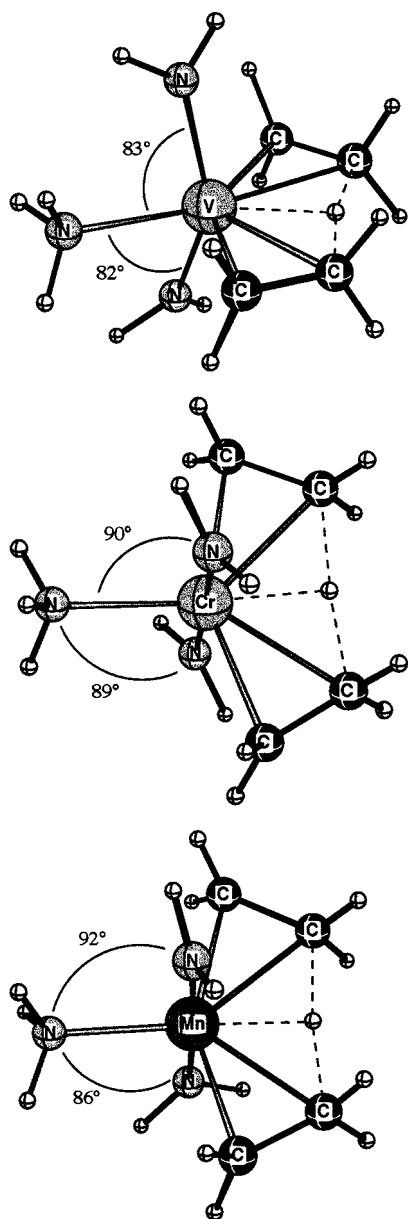


Fig. 7. Shapes of BHT, the β -hydride transfer transition state.

linking the amine to each of the amides as depicted in Scheme 3.

With the ethyl bridges, the three nitrogens orient themselves either on one face of the metal (with an amide–M–amide angle of 123–134°) or along a meridian (with an amide–M–amide angle of 155–160°). This restricted geometry of the chelating ligand facilitates the uptake of ethylene by keeping a coordination site accessible on the other side of the metal. The ethyl tethers also restrict the rotations of the amide groups, significantly changing the reaction profiles by changing the overlap of the V and Cr systems' π bonds. Steric bulk in this system is still very small, allowing us to continue to focus on the electronic effects. The energetics

calculated for catalysis in these systems is summarized in Table 4.

In each case we compare the results to those of the generic systems in Table 1.

The uptake energy, E_{OC} , was substantially improved in the V and Cr cases. E_{OC} is the difference between the energy of the precursor and the olefin adduct, so we will examine the changes the addition of the ethyl tethers makes in both. The chelating ligand is well suited to a trigonal bipyramidal shape, with the two amide–M–amine angles restricted to less than 90° and the amide–M–amide angle at just over 120°, so for all three metals the five-coordinate olefin adduct will be substantially energetically favored in comparison to the four-coordinate, pseudo-tetrahedral precursor. To estimate the energy required to bend the other ligands back to accommodate the incoming olefin, an additional single point calculation was done for each metal using the optimized geometry of the system after ethylene uptake — except that the ethylene was omitted. The difference between this energy and the energy of the fully optimized precursor is an estimate of the energy required to distort the other ligands to accommodate the incoming ethylene, and is labeled $\Delta E_{reorganization}$ in Table 5.

The binding energy, $\Delta E_{OC} - \Delta E_{reorganization}$, olefin would have if the other ligands were held in the same orientation in the precursor that they have after ethylene uptake is about 20 kcal mol⁻¹ in each case. To understand the causes of the differences in E_{OC} ener-

Table 3

Calculated reaction enthalpies (in kcal mol⁻¹) for second-row element systems

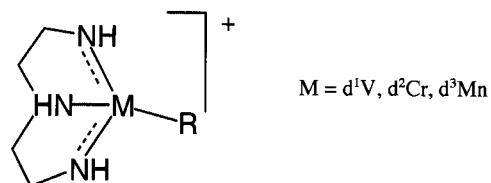
Model catalyst	E_{OC} ^a	ΔE_{INS}^\ddagger ^b	ΔE_{BHT}^\ddagger ^c
(NH ₂) ₂ Mo(C ₂ H ₅) ⁺	^d	+25	+19.6
(NH ₂) ₂ Ru(C ₂ H ₅) ⁺	-38.9	+30	+31.0
(NH ₂) ₂ Pd(C ₂ H ₅) ⁺	-14.3	+19.3	+23.3
(NH ₂) ₂ NH ₃ Mo(C ₂ H ₅) ⁺	-18.7	+23.8	+25.2
(NH ₂) ₂ NH ₃ Ru(C ₂ H ₅) ⁺	-38.9	+25	^d
(NH ₂) ₂ NH ₃ Pd(C ₂ H ₅) ⁺	-14.3	+19.3	+21.0

^a Energy of olefin coordinated compound with respect to ethylene and precursor.

^b Barrier height — energy of ethylene insertion TS with respect to OC.

^c Barrier height — energy of β -hydride transfer TS with respect to OC.

^d Results not obtained.



Scheme 3. Model of chelating ligand systems.

Table 4
Energies (in kcal mol⁻¹) of systems with chelating ligand

Model system	Energy with respect to reactants			Barrier heights	
	E_{OC}^a	E_{INS}^\ddagger ^b	E_{BHT}^\ddagger ^c	ΔE_{INS}^\ddagger ^d	ΔE_{BHT}^\ddagger ^e
LVCH ₂ CH ₃ ⁺	-9.9	4.2	-1.2	+5.7	+8.7
LCrCH ₂ CH ₃ ⁺	-15.3	-3.2	+10.2	+12.1	+25.6
LMnCH ₂ CH ₃ ⁺	-3.2	+6.4	+15.5	+9.6	+18.8

L = HNCH₂CH₂N(H)CH₂CH₂NH.

^a Energy of olefin coordinated compound with respect to ethylene and precursor.

^b Energy of ethylene insertion TS with respect to ethylene and precursor.

^c Energy of β -hydride transfer TS with respect to ethylene and precursor.

^d Barrier height — energy of ethylene insertion TS with respect to OC.

^e Barrier height — energy of β -hydride transfer TS with respect to OC.

gies, we examine the effect the tethers have on the energies of OC isomers. Ideally, the tether should hold the nitrogens in the shape they have in the generic system OC complexes. The less the generic system (as shown in Fig. 3) needs to be distorted to accommodate the chelating ligand, the more stable the chelated OC system will be and the greater the ethylene binding energy. The OC isomer of Cr is already very near to the shape it must assume with the chelating ligand, with the three nitrogens on one face of Cr and with the amides each directing a hydrogen at the amine. Thus the reorganization costs only 3.7 kcal mol⁻¹ for Cr with the chelating ligand, resulting in an excellent E_{OC} of -15.3 kcal mol⁻¹. The generic V system is nicely facial, but with tethered system the amides cannot rotate themselves to avoid sharing a π orbital. The chelating ligand twists to partially avoid this overlap, resulting in R-N-V-N torsions of -33.8 and 44.2°. The V system prefers to have one of them be zero, as shown in Table 2. This results in a higher reorganization energy, and thus a lower olefin affinity, with an E_{OC} of -9.9 kcal mol⁻¹. The generic system Mn OC orients an amine *trans* to an amide, but since the tethered system cannot do this, its reorganization energy is quite high, resulting in a poor E_{OC} of -3.2 kcal mol⁻¹.

Similarly, the suitability of the generic analogue system to form a chelate correlates to the energetics of the insertion process. We see in Fig. 5 that both the V and Cr generic systems are well suited to the attachment of a tether, resulting in similar low E_{INS} values for the two systems. The barrier height (ΔE_{INS}^\ddagger) is relative to the OC structure, so the Cr case has a higher barrier than the V because the Cr OC system is significantly lower in energy than the V OC. With significantly negative E_{INS} enthalpies, these model systems would be active catalysts. The Mn INS transition state, like the Mn OC structure, is high in energy because the chelating ligand does not allow it to assume a shape like its generic analogue, with an amine *trans* to an amide.

Finally, the BHT transition state is quite different. For vanadium, the nitrogens in the generic system shown in Fig. 7 are quite suitable for the chelating ligand system, so the E_{BHT} is fairly low. The chromium case is very different — the chromium prefers to orient the amides *trans* to one another, and share both their σ and π orbitals, as shown in Fig. 2. The chelating ligand flattens out to a pseudo-meridional shape, but the amide-Cr-amide angle can only widen to 155°. This lowers the overlap of the σ - and π -bonding interactions of chromium, weakening the bonds and causing a large energy penalty for this conformer with respect to the generic system and a very high ΔE_{BHT} . The chelating Mn system also is pseudo-meridional shape with a less than linear amide-Cr-amide angle (158°), also resulting in a high E_{BHT} .

Overall, the results of the calculations on this chelating system are very encouraging. Although the Mn case was poor, both the vanadium and chromium have low E_{INS} values, which is necessary for rapid polymerization. The energy difference between the insertion and termination barriers determines the average polymer chain length; for the vanadium system it was 3 kcal mol⁻¹. For a system with such little steric bulk it is expected that this would be low; in many unhindered systems it is actually negative [3,7,8,33] but adding

Table 5

Energy required to distort the precursor to accommodate the incoming ethylene (energies in kcal mol⁻¹)

Model system	E_{OC}^a	$\Delta E_{reorganization}^b$	$\Delta E_{OC} - \Delta E_{reorganization}^c$
LVCH ₂ CH ₃ ⁺	-9.9	+11.8	-21.7
LCrCH ₂ CH ₃ ⁺	-15.3	+3.7	-19.0
LMnCH ₂ CH ₃ ⁺	-3.2	+16.4	-19.6

^a Energy of olefin coordinated compound with respect to ethylene and precursor.

^b Energy of OC geometry with ethylene group omitted with respect to precursor.

^c This difference is what E_{OC} would be if the ligand and alkyl were prearranged to facilitate uptake.

steric bulk can raise it considerably. The chromium system has an exceptionally high termination barrier, 13.5 kcal mol⁻¹ higher than its insertion barrier. Such a large gap between insertion and termination is consistent with a living catalyst.

4. Conclusions

This computational exploration of transition metals with intermediate electron counts indicates several potentially active olefin polymerization catalysts, particularly for chromium(IV) species. Localized orbitals provide an intuitive, simple visualization tool for describing these structures. We find that as we change metals, the change in the number of singly occupied metal orbitals causes dramatic differences in the shapes of the stationary points in the catalytic cycle. The change in the number of metal bonding orbitals causes these differences. Unfortunately, we find that these simple generic models have low olefin uptake energies and sizeable insertion barriers. Second-row transition metal analogues to these amide/amine systems are also briefly examined and were not found to be promising.

Introducing two ethyl tethers to the system to form a chelating ligand has a dramatic positive effect on the olefin polymerization properties of the vanadium and chromium catalysts. Because the preferred shapes of the different stationary points were quite different, the geometry restrictions caused by the tethers have different energetic effects on different stationary points. By choosing a ligand system where the preferred termination geometry is inaccessible while encouraging the insertion by holding the ligands in a position ideal for insertion, the catalytic properties are vastly improved in the Cr case, both in uptake energy and in a large increase in the termination barrier. The 13.5 kcal mol⁻¹ difference between the insertion and termination barriers makes it a good candidate for a high molecular weight catalyst. A low insertion barrier of 5.7 kcal mol⁻¹ is predicted for the vanadium case, making it a good polymerization catalyst candidate; further modification of the ligand system to add steric bulk may increase the termination barrier and increase the expected molecular weight of the polymer.

Acknowledgements

This investigation was supported by the Natural Sciences and Engineering Research Council of Canada (NSERC) and by Novacor Research and Technology Corporation. We thank Jochen Autschbach for helpful discussions about molecular orbital manipulation and display.

References

- [1] H. Schnutenhaus, H.H. Brintzinger, *Angew. Chem. Int. Ed. Engl.* 18 (1979) 77.
- [2] (a) J.C. Stevens, F.J. Timmers, D.R. Wilson, G.F. Schmidt, P.N. Nicklas, R.K. Rosen, G.W. Knight, S.Y. Lai, *Eur. Pat. Appl. EP*, 416815, 1990;
(b) J.C. Stevens, D.R. Neithammer, *Eur. Pat. Appl. EP*, 418044, 1990;
(c) J.A.M. Canich, *Eur. Pat. Appl. EP*, 420436, 1990.
- [3] J.D. Scollard, D.H. McConville, N.C. Payne, J.J. Vittal, *Macromolecules* 29 (1996) 241.
- [4] M. Bochmann, *J. Chem. Soc. Dalton Trans.* (1996) 255.
- [5] (a) C.A. Jolly, D.S. Marynick, *J. Am. Chem. Soc.* 111 (1989) 968;
(b) L.A. Castonguay, A.K. Rappé, *J. Am. Chem. Soc.* 114 (1992) 5832;
(c) H. Kawamura-Kuribayashi, N. Koga, K. Morokuma, *J. Am. Chem. Soc.* 114 (1992) 2359;
(d) H. Kawamura-Kuribayashi, N. Koga, K. Morokuma, *J. Am. Chem. Soc.* 114 (1992) 8687;
(e) H. Weiss, C. Ehrig, R. Ahlrichs, H. Kawamura-Kuribayashi, N. Koga, K. Morokuma, *J. Am. Chem. Soc.* 116 (1994) 4919;
(f) T.K. Woo, L. Fan, T. Ziegler, *Organometallics* 13 (1994) 432;
(g) T.K. Woo, L. Fan, T. Ziegler, *Organometallics* 13 (1994) 2252;
(h) T. Yoshida, N. Koga, K. Morokuma, *Organometallics* 14 (1995) 746;
(i) J.C.W. Lohrenz, T.K. Woo, T. Ziegler, *J. Am. Chem. Soc.* 117 (1995) 12793;
(j) T.K. Woo, P.M. Margl, J.C.W. Lohrenz, P.E. Blöchl, T. Ziegler, *J. Am. Chem. Soc.* 118 (1996) 13021.
- [6] (a) P. Margl, L. Deng, T. Ziegler, *Organometallics* 17 (1998) 933;
(b) P. Margl, L. Deng, T. Ziegler, *J. Am. Chem. Soc.* 120 (1998) 5517;
(c) P. Margl, L. Deng, T. Ziegler, *J. Am. Chem. Soc.* 121 (1999) 154;
(d) P. Margl, L. Deng, T. Ziegler, *Top. Catal.* 7 (1999) 187.
- [7] (a) L.K. Johnson, C.M. Killian, M. Brookhart, *J. Am. Chem. Soc.* 117 (1995) 6414;
(b) L.K. Johnson, S. Mecking, M. Brookhart, *J. Am. Chem. Soc.* 118 (1996) 267;
(c) C.M. Killian, D.J. Tempel, L.K. Johnson, M. Brookhart, *J. Am. Chem. Soc.* 118 (1996) 11664;
(d) F.C. Rix, M. Brookhart, P.S. White, *J. Am. Chem. Soc.* 118 (1996) 4746.
- [8] (a) L. Deng, P.M. Margl, T. Ziegler, *J. Am. Chem. Soc.* 119 (1997) 1094;
(b) L. Deng, T.K. Woo, L. Cavallo, P.M. Margl, T. Ziegler, *J. Am. Chem. Soc.* 119 (1997) 6177;
(c) R.D.J. Froese, D.G. Musaev, K. Morokuma, *J. Am. Chem. Soc.* 120 (1997) 1581;
(d) D.G. Musaev, R.D.J. Froese, K. Morokuma, *Organometallics* 17 (1998) 1850.
- [9] S.D. Ittel, L.K. Johnson, M. Brookhart, *Chem. Rev.* 100 (2000) 1169.
- [10] G.J.P. Britovsek, V.C. Gibson, D.F. Wass, *Angew. Chem. Int. Ed. Engl.* 38 (1999) 428.
- [11] F.J. Karol, G.L. Karapinka, C. Wu, A.W. Dow, R.N. Johnson, W.L. Carrick, *J. Polym. Sci. Part A-1* 10 (1972) 2621.
- [12] J.P. Hogan, R.L. Banks (Phillips Petroleum), US patent 2825721; *Chem. Abstr.* 52 (1958) 8621h.
- [13] K.H. Theopold, *Eur. J. Inorg. Chem.* (1998) 15.
- [14] (a) B.J. Thomas, S.K. Noh, G.K. Schulte, S.C. Sendlinger, K.H. Theopold, *J. Am. Chem. Soc.* 113 (1991) 893;

- (b) G. Bhandari, Y. Kim, J.M. McFarland, A.L. Rheingold, K.H. Theopold, *Organometallics* 14 (1995) 738;
(c) P.A. White, J. Calabrese, K.H. Theopold, *Organometallics* 15 (1996) 5473.
- [15] R. Emrich, O. Heinemann, P.W. Jolly, C. Krüger, G.P.J. Verhovnik, *Organometallics* 16 (1997) 1511.
- [16] (a) W.-K. Kim, M.J. Fevola, L.M. Liable-Sands, A.L. Rheingold, K.H. Theopold, *Organometallics* 17 (1998) 4541;
(b) P.H.M. Budzelaar, A.B. van Oort, A.G. Orpen, *Eur. J. Inorg. Chem.* (1998) 1485.
- [17] (a) V.C. Gibson, C. Newton, C. Redshaw, G.A. Solan, A.P.J. White, D.J. Williams, *J. Chem. Soc. Dalton Trans.* (1999) 827;
(b) V.C. Gibson, S. Mastroianni, C. Newton, C. Redshaw, G.A. Solan, A.P.J. White, D.J. Williams, *J. Chem. Soc. Dalton Trans.* (2000) 1969.
- [18] R.D. Köhn, M. Haufe, G. Kociok-Köhn, S. Grimm, P. Wasserscheid, W. Keim, *Angew. Chem. Int. Ed. Engl.* 39 (2000) 4337.
- [19] R.D. Köhn, M. Haufe, S. Mihan, D. Lilge, *Chem. Commun.* (2000) 1927.
- [20] R. Schmid, T. Ziegler, *Organometallics* 19 (2000) 2756.
- [21] L. Deng, R. Schmid, T. Ziegler, *Organometallics* 19 (2000) 3069.
- [22] M.J.S. Dewar, *Bull. Soc. Chim. France* 18 (1951) C71.
- [23] (a) ADF 2.3.3, Theoretical Chemistry, Vrije Universiteit, Amsterdam;
(b) E.J. Baerends, D.E. Ellis, P. Ros, *Chem. Phys.* 2 (1973) 41.
- [24] G. te Velde, E.J. Baerends, *J. Comput. Phys.* 99 (1992) 84.
- [25] J.G. Snijders, E.J. Baerends, P. Vernoijs, *At. Nucl. Data Tables* 26 (1982) 483.
- [26] J. Krijn, E.J. Baerends, *Fit Functions in the HFS Method*, Department of Theoretical Chemistry, Free University, Amsterdam, The Netherlands, 1984.
- [27] S.H. Vosko, L. Wilk, M. Nusair, *Can. J. Phys.* 58 (1980) 1200.
- [28] A. Becke, *Phys. Rev. A* 38 (1988) 3098.
- [29] (a) J.P. Perdew, *Phys. Rev. B* 34 (1986) 7406;
(b) J.P. Perdew, *Phys. Rev. B* 34 (1986) 8822.
- [30] (a) P. Margl, T. Ziegler, *Organometallics* 15 (1996) 5519;
(b) P.M. Margl, T. Ziegler, *J. Am. Chem. Soc.* 118 (1996) 7337.
- [31] B. Jensen, K. Børve, *J. Comput. Chem.* 19 (1998) 947.
- [32] (a) J.G. Snijders, E.J. Baerends, *Mol. Phys.* 36 (1978) 1789;
(b) J.G. Snijders, E.J. Baerends, P. Ros, *Mol. Phys.* 38 (1979) 1909.
- [33] L. Deng, T. Ziegler, T. Woo, P. Margl, L. Fan, *Organometallics* 17 (1998) 3240.
- [34] J. Autschbach, ADFPLT 1.1 program, 2000. Enquiries may be sent to jochen@cobalt78.chem.ucalgary.ca.
- [35] C.R. Landis, T.K. Firman, D.M. Root, T. Cleveland, *J. Am. Chem. Soc.* 120 (1998) 1842.
- [36] (a) C. Edmiston, K. Rüdénberg, *Rev. Mod. Phys.* 35 (1963) 457;
(b) S.F. Boys, *Rev. Mod. Phys.* 32 (1960) 253;
(c) W. von Niessen, *J. Chem. Phys.* 47 (1967) 253.